JPPIPA 9(9) (2023)

Jurnal Penelitian Pendidikan IPA

Journal of Research in Science Education

http://jppipa.unram.ac.id/index.php/jppipa/index

The Influence of Electrospinning Process Parameters of Polyvinylidene Fluoride and Polyacrylonitrile (PVDF/PAN) Nanofiber Composites

Ida Sriyanti[1,4,*], Muhammad Rama Almafie[1,2,4], Rahma Dani[1,4], Meutia Kamilatun Nuha Ap Idjan[3], Radiyati Umi Partan[3], M Rudi Sanjaya[4], Jaidan Jauhari[4]

[1]Physics Education, Faculty of Education, Universitas Sriwijaya, Indralaya, Indonesia.
[2]Mathematics and Natural Sciences, Faculty of Mathematics and Natural Sciences, Universitas Sriwijaya, Indralaya, Indonesia.
[3]Medicine, Faculty of Medicine, Universitas Sriwijaya, Indralaya, Indonesia.
[4]Electronic and Nanotechnology Applications Research Group, Faculty of Computer Science, Universitas Sriwijaya, Palembang, Indonesia.

Received: July 31, 2023
Revised: September 16, 2023
Accepted: September 25, 2023
Published: September 30, 2023

Corresponding Author:
Ida Sriyanti
ida_sriyanti@unsri.ac.id

DOI: 10.29303/jppipa.v9i9.4840

Abstract: PAN cannot be used as a stand-alone nanofiber, so it needs to be modified through copolymerization with other polymers, such as PVDF. It is composite mutually beneficial for both PVDF/PAN polymers. Study aims to see the effect of process parameters, such as voltage, flow rate and needle tip distance of PVDF/PAN composite nanofiber as well as molecular interaction and crystal structure, to confirm the presence of polymer in the nanofiber composite. The nanofibers with solution parameters PN1: PVDF 6% and PAN 8%, PN2: PVDF 6% and PAN 10%, and PN3: PVDF 6% and PAN 12% were prepared using electrospinning. Morphology of the process parameters of voltage (12kV, 16kV, 18kV), flow rate (30 µl/min, 60 µl/min, 90 µl/min) and needle tip distance (75 mm, 100 mm, 125 mm) were observed. The results showed straight and continuous fibre morphology, with a smooth surface and no beaded structure, with homogeneous fibre distribution with an increase in diameter from 394 ± 79 nm (NF1) to 851 ± 89 nm (NF3). The optimal state was in the solution of PN2: PAN 10% (w/w) and PVDF 6% (w/w), High Voltage 12 kV, Flow Rate PN3: 60 µl/min, and Needle to Collector Distance 75 mm.

Keywords: Concentration; Distance tip; Flow rate; High voltage; Homogeneity

Introduction

Nanotechnology is revolutionizing society by changing how we manufacture and design for the future. Nanoparticles range in size from 1 to 100 nm on average and are controlled aggregates of atoms or matter. (Khan, Saeed, & Khan, 2019). Due to its appealing features, tiny dimensional area, high aspect ratio, numerous possible uses, and degree of flexibility, one-dimensional (1D) nanostructured materials are gaining interest. 1D nanomaterials, including nanofiber, nanowire and polymer combinations, have received much attention in nanoscale applications (Machín et al., 2021). Their efficiency is further increased by the structural regularity of nanofiber and nanofiber mat, which have tiny fibre diameters and high specific surface area to volume ratios. Nanofibers feature tiny fibre diameters, high porosity, and sophisticated chemical characteristics, including permeability and porosity (Islam, Ang, Andriyana, & Afifi, 2019; Kenry & Lim, 2017; Lee, Bui-Vinh, Baek, Kwak, & Lee, 2023). They can be selectively manufactured and control the pore size based on application requirements. Additionally, all requirements for capturing fine particles can be met by adding substances and particles and altering the morphology of nanofibers. Nanofibers are ideal for membrane filtration technology, tissue regeneration and biomedical engineering, sensor and electronic device applications, as well as the smart textile industry. These benefits include better mechanical stability, higher air

How to Cite:
Sriyanti, I., Almafie, M.R., Dani, R., Idjan, M.K.N.A., Partan, R.U., Sanjaya, M.R., & Jauhari, J. (2023). The Influence of Electrospinning Process Parameters of Polyvinylidene Fluoride and Polyacrylonitrile (PVDF/PAN) Nanofiber Composites. *Jurnal Penelitian Pendidikan IPA*, *9*(9), 7159–7169. https://doi.org/10.29303/jppipa.v9i9.4840

permeability due to their slip-flow effect, and good electrostatic effect.

Adding particles and composites can also produce many nanofibers with unique properties. Polysaccharides, collagen, silk, cellulose, and synthetic polymers like polyacrylonitrile (PAN) may all be easily formed into nanofibers (Sanchaniya & Kanukuntla, 2023; Thorat, Chavan, & Mohite, 2022), poly(lactic acid), and polyvinyl alcohol (PVA) (Kusumawati, Istiqomah, Husnia, & Fathurin, 2021), Polyvinylidene fluoride (PVDF) (Russo et al., 2020; Saha, Yauvana, Chakraborty, & Sanyal, 2019), Polyvinylpyrrolidone (PVP) (Latiffah, Agung, Hapidin, & Khairurrijal, 2022) and Polyethersulfone (PESU) (Al-Husaini, Lau, Yusoff, Al-Abri, & Farsi, 2021). PVDF is an essential material in manufacturing tactile sensors and energy harvesters, which is popular due to its piezoelectric properties (Julius, 2012). PVDF is semi-crystalline, with a percentage crystallinity of about 50-70%, resulting in a sandwiched structure of crystalline and amorphous areas. PVDF promises high mechanical strength, good chemical resistance, high dielectric constant, excellent thermal stability and ageing resistance. The [-(CF_2-CH_2)n-] backbone of PVDF induces dipole moments due to the strong electronegativity of fluoro atoms compared to hydrogen or carbon atoms(Li, Liao, & Tjong, 2019). On the other hand, PAN is a white semi-crystalline synthetic organic polymer. The majority of chemical and inorganic solvents cannot dissolve the polymer. PAN is a thermoplastic polymer with excellent chemical resistance, heavy metal adsorption and mechanical properties, and lithium fibre. However, PAN morphology and mechanical properties decrease as the plasticizer content increases. PAN cannot be used as a stand-alone nanofiber; it must be modified through copolymerization with other polymers, such as PVDF. This composite is mutually beneficial for both PVDF/PAN polymers.

Nanofibers can be produced using electrospinning, offering high production rates at low cost. Electrospinning equipment with needles, spinners, and collectors is designed for optimal nanofiber structures in targeted applications (Xue, Wu, Dai, & Xia, 2019). The most popular arrangement on the market currently includes a syringe pump, a high-voltage DC power source, and a collector. Through the relevant factors, this configuration will impact the morphological formation that needs to be established throughout the electrospinning process. The concentration of the polymer solution, viscosity, conductivity, and surface tension are among the solution properties (Agarwal, Greiner, & Wendorff, 2013; Collins, Federici, Imura, & Catalani, 2012; Reneker, Yarin, Fong, & Koombhongse, 2000; Tan, Inai, Kotaki, & Ramakrishna, 2005). Significant structures like particles, beads, and nanofibers will be produced due to the impacts of attention and viscosity. An increase in polymer concentration causes increased solution viscosity, a decrease in the number of grains, and the production of uniform fibres. Voltage, tip-to-collector separation, and polymer solution feed rate are processing parameters used in electrospinning. In some cases, nanofibers can be produced after overcoming a threshold pressure, which causes a significant charge difference in the solution (Al-Abduljabbar & Farooq, 2023). Another crucial element is the polymer solution flow rate, with lower flow rates ensuring complete solvent evaporation from the nanofiber. The collector and distance tip also govern the spherical fibres diameter and morphology.

Research involving PVDF and PAN to observe morphology has been widely conducted in recent years, for example, PVDF-Chiotan-gelatin nanocomposites as a potential application in wound dressing. They used a 5%-25% (w/v) solution parameter formulation to produce bead and large fibre morphology (Mohseni, Delavar, & Rezaei, 2021). PAN/Graphene composites can be used as electrodes in energy storage and have high dielectric properties. The resulting nanofiber has a characteristic bead-free morphology with a fixed solution concentration of 10% (w/w) with increasing graphene mass (Almafie et al., 2022). AgNO3-PAN/PVDF composites were applied to air permeability, where the solution was adjusted in the concentration of polymer ratio of 60-80%, PVDF 20-30% and $AgNO_3$ 0-20% resulting in fibre morphology such as strands of hair in diameter (Ince Yardimci, Durmus, Kayhan, & Tarhan, 2022). However, they have not specifically optimized the parameters of the electrospinning process so that a homogeneous and smooth diameter is produced. The research focuses on the solution parameters based on these investigations. Therefore, the influence of process parameters, such as voltage, flow rate and distance tip to needle, must be investigated through morphology observation. As well as molecular interactions and crystal structure to confirm the presence of polymer in the nanofiber composite.

Method

Material

Polyacrylonitrile (PAN, MW 150,000 kg/mol, and Polyvinylidene fluoride (PVDF, MW 180,000 kg/mol, CAS 24937-79-9) were purchased from Sigma-Aldrich (Singapore). N,N-Dimethylformamide (DMF, ≥99.8% Assay, CAS 68-12-2) VWR Chemicals BDH (Singapore). All reactants were used as received without further treatment (analytical grade).

Preparation of Solution Parameters

PVDF/PAN composite nanofiber was prepared from a mixture of PVDF and PAN polymers in the same container using DMF non-polar solvent. Details of the solution composition expressed in variable concentrations are given in Table 1. The PVDF/PAN dispersion was heated on a Hotplate Magnetic Stirrer (Thermo Scientific, Singapore) for approximately 12 hours at 80°C with a stirring speed of 300 rpm to obtain a uniform spinning solution. The electrospinning procedure utilised Nachriebe 601 ITB (Bandung, Indonesia). Put the prepared solution into an 8 mL plastic syringe connected to a No. 16 G stainless steel needle as a nozzle. The syringe was driven by a pump with a 30 µl/min flow rate. A voltage of 10 kV was applied to perform electrospinning. The distance tip and the collector were constant at 75 mm. A grounded drum collector wrapped with aluminium foil collected the fibres. After electrospinning, the electrospun nanofibrous mat was carefully removed from the aluminium foil and dried in a vacuum overnight at room temperature.

Table 1. Composition of the prepared PVDF/PAN.

Label	PVDF (%.w/w)	PAN (%.w/w)	DMF (%.w/w)
PN1	6	8	86
PN2	6	10	84
PN3	6	12	82

Preparation of Process Parameter

The optimum polymer solution is introduced into the syringe. The needle is wired to the positive end of the high-voltage source. The entire assembly is put in a room with a securely closed door, and variable high voltage between 12 and 18 KV is delivered. the variable flow rate was applied at 30-90/min while the nozzle that formed the Taylor cone was deposited on a metal collector wrapped in aluminium foil. This flow rate was adjusted to control the release rate of the polymer solution. the variable distance tip and collector were utilized at a distance of 75-125 mm, allowing the solution to produce an intact fibre extension.

Characterization of Nanofiber

Using a scanning electron microscope (SEM, JEOL JSM-6510 LA, Japan) and a fluorescence microscope (MF, Optika, B-380 MET, Italy) were explicitly used to observe the samples at the solution parameter stage and the process parameter stage, respectively, the morphology of the nanofibers was examined. Each sample was calculated for diameter, standard deviation, and homogeneity using Image J 1.54 (National Institutes of Health, US). FTIR spectroscopy (FTIR, 8201PC Shimadzu, Japan) was used to evaluate and identify intermolecular bonds and functional groups in each sample. IR absorption peaks were studied using FTIR at 400 to 4000 cm-1 wavelengths. The nanofiber scaffold's structure and crystal shape were examined using X-ray diffraction (XRD). The scanning range was 5°–60°, the scanning voltage was 40 kV, and the scanning current was 40 mA. The speed rate was 5°/min.

Result and Discussion

Nanofiber PVDF/PAN

Morphology and distribution of PVDF/PAN nanofiber produces fine fibres with a thin surface area, as shown in Figure 1. The resulting nanofiber are homogeneous despite adding non-polymeric substances that can reduce homogeneity. Electrospinning successfully converted the PVDF/PAN composite solution into nanofibers. In the electrospinning process, a push with a set flow rate will push the difficulty until the solution comes out towards the tip of the needle.

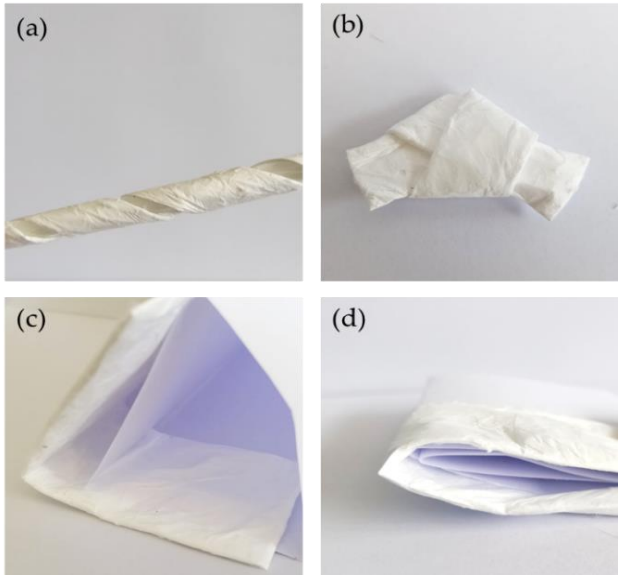

Figure 1. The optical photos of PN1.

A high-voltage source is connected to the distance tip of the needle, giving a positive charge and the collector a negative charge. The charge at the distance tip of the needle will induce the solution. Taylor cone jet will be formed when the amount of charge loads with surface tension. If the charge contained exceeds the surface tension, there is emission from the tip of the needle, causing the solution to come out through the distance tip. The charge jet is drawn and gathers on the surface of the collector drum. The nanofiber exhibits curved flexibility and can be easily rolled into a helix, cooled, and self-rotated, allowing it to be folded into various angles with external support. After removing the force,

it will quickly reflect on the prototype without leaving a crease.

SEM analysis

The surface morphology of PVDF/PAN nanofiber of PN1, PN2, and PN3 as a function of concentration showed that the nanofiber microstructure was straight and continuous, with a smooth surface and no beaded structure, as shown in the scanning electron micrograph in Figure 2. The histogram shows that increasing PAN concentration influences the diameter of the nanofibers. As the PAN concentration increased from 8% to 12%, the diameter increased from 394 ± 79 nm (NF1) to 851 ± 89 nm (NF3). The distribution of nanofibers is categorized as homogeneous because the coefficient of variation (σ) is smaller than 0.3 (Jauhari, Wiranata, Rahma, Nawawi, & Sriyanti, 2019; Sriyanti, Marlina, Fudholi, Marsela, & Jauhari, 2021). Although in previous studies, the average diameter of pure PVDF and pure PAN nanofibers were around 328 ± 108 nm and 443 ± 75 nm, respectively, when the concentration was less than 10% (Gade, Nikam, Chase, & Reneker, 2021; Jauhari, Suharli, Nawawi, & Sriyanti, 2021). The viscosity and surface tension increase in solution is directly proportional to the polymer concentration. A high viscosity indicates the extent to which the polymer molecular chains are bound in solution, resulting in larger fibres. Conversely, solutions with low viscosity produce smaller fibres or granules.

High viscosity bonds between polymer molecular chains prevent secondary emission or double emission caused by charge interactions(Eren Boncu, Ozdemir, & Uskudar Guclu, 2020; Prabu & Dhurai, 2020; Sengor, Ozgun, Gunduz, & Altintas, 2020). Surface tension is the attractive force acting on molecules on the surface of a liquid, forming the smallest specific surface area. In high-viscosity solutions, the interaction between polymer and solvent molecules is more dominant than between solvent molecules. This causes the solvent molecules to spread around the polymer molecules and not form a roundabout when attracted to the electric voltage. In contrast, in a low-viscosity solution, the number of solvent molecules is greater than that of polymer molecules, causing a more dominant interaction between the solvent molecules and the sphere(Ahmadian, Shafiee, Aliahmad, & Agarwal, 2021; Liang, Pan, & Gao, 2021; Wang & Nakane, 2020). Fibres can still form when the solution is drawn into the collector, but due to the large surface tension, these fibres form small spheres or beads.

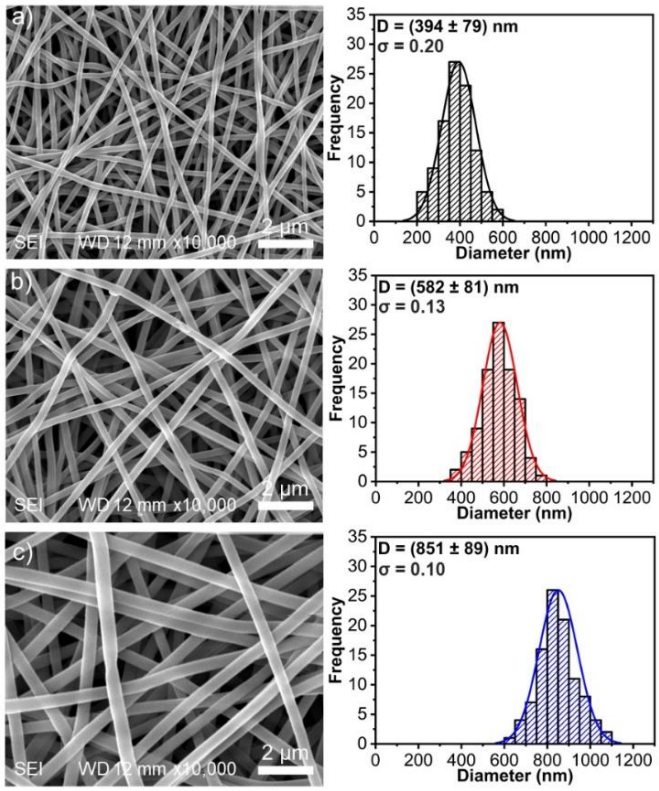

Figure 2. Morphology and Distribution of PVDF/PAN Composite Nanofiber of (a) PN1, (b)PN2, and (c) PN 3 as the Effect of Concentration Variables.

PN1 nanofiber solution with 6% (w/w) PVDF and 10% (w/w) PAN concentration was selected as the most optimum fibre composition to analyze the electrospinning process parameters. This is based on the homogeneous continuous ribbon-like shape of the nanofiber, and the size is manageable. The morphology and distribution of PVDF/PAN nanofibers as an effect of voltage were observed using MF, which can be seen in Figure 3. The voltage variation was set at 12 kV, 16 kV and 18 kV. The flow rate and distance between the nozzle and collector were kept constant at 30 µl/min and 75 mm, respectively. Each nanofiber was observed to be bead-free, with no defects in a regular state, but had differences in fibre size and homogeneity. These results align with previous studies that the effect of voltage variation does not change the regularity of the nanofibers (Ghafouri et al., 2022; Jadbabaei, Kolahdoozan, Naeimi, & Ebadi-Dehaghani, 2021; Mahdavi Varposhti, Yousefzadeh, Kowsari, & Latifi, 2020). The average diameter affected by a high voltage at 12 kV, 16 kV, and 18 kV was 647 ± 185 nm, 598 ± 149 nm, and 538 ± 143 nm and fibre homogeneity with a coefficient of variance (σ) values of 0.26, 0,.9, and 0.33, respectively. Where PN1 and PN2 are set homogeneous, and PN3 is set inhomogeneous.

Higher stress usually leads to more excellent solution stretching due to the coulomb force and electric

field on the stronger jet(Liyanage, Biswas, Dalir, & Agarwal, 2023). This has the effect of reducing the fibre diameter and promoting solvent evaporation to produce drier fibres. When a low-viscosity solution is used, higher tension can favour the formation of secondary jets during electrospinning, thus reducing fibre diameter(Rathore & Schiffman, 2021; Xu, Lv, Wang, & Qu, 2023). At lower voltages, the jet acceleration is reduced, and the weak electric field can increase the electrospinning jet flight time, favouring fine fibre formation. In this case, a voltage close to the critical voltage for electrospinning is advantageous to obtain finer fibres.

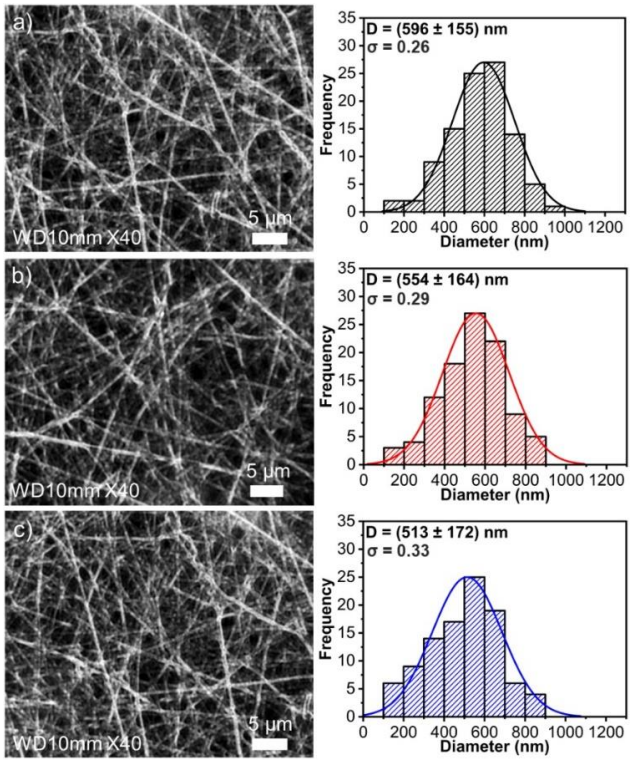

Figure 3. Morphology and Distribution of PVDF/PAN Composite Nanofiber of (a) PN3: 12 kV, (b) PN3: 16 kV dan (c) PN3:18 kV as the Effect of High Voltages Variables.

The morphology and size of PVDF/PAN nanofiber as an effect of variable flow rate obtained from SEM images are presented in Figure 4. The voltage rate variation was set at 30 µl/min, 60 µl/min and 90 µl/min. The flow rate was set at 10 kV, and the distance between the nozzle and collector was constant and 75 mm. PN1 nanofiber: 30 µl/min had a smooth and uniform surface with a 647 ± 185 nm diameter. The nanofiber mat with PN1: 60 µl/min has a rough and beadless surface with a diameter of 598 ± 149 nm, while and has a more uniform structure than the PN1 nanofiber mat: 80 µl/min with a diameter of 538 ± 143 nm. In addition, the comparison analysis between the standard deviation and the average diameter confirmed that the nanofibers remained homogeneous (σ<0.3). The flow rate increases the amount of polymer solution available for spinning, resulting in larger fibres. A stable Taylor cone requires a specific flow rate, but high flow rates can cause the polymer solution to fall or drip from the needle tip, preventing fibre formation(Baykara & Taylan, 2021; Gelb et al., 2022). Increasing the solution flow rate can increase the fibre's size and the number of ions or free charges per unit volume. This increased force causes more excellent tensile and elongation due to charge interactions(He, Rault, Lewandowski, Mohsenzadeh, & Salaün, 2021; Jiang et al., 2020). The increase in fibre size is balanced by an increase in fibre tension and elongation, ensuring that the fibre size does not increase significantly.

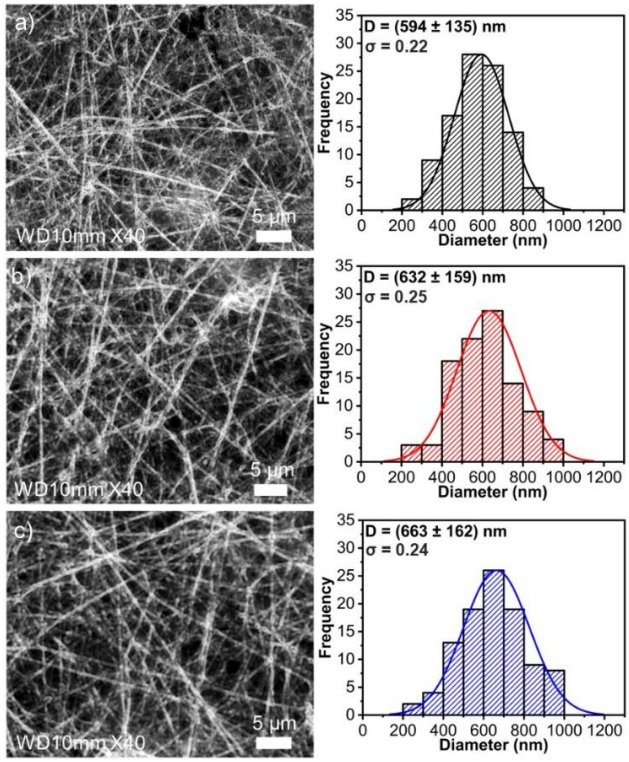

Figure 4. Morphology and Distribution of PVDF/PAN Composite Nanofiber of pada (a)PN3: 30 µl/min, (b)PN3: 60 µl/min dan (c)PN3: 90 µl/min as the Effect of Flowrate Variables.

MF images of PVDF/PAN nanofibers with different needle-to-collector distances are shown in Figure 5. The morphology of the nanofibers after crosslinking showed no significant difference except for an increase in fibre diameter, as evidenced by the diameter distribution histogram. At 75 mm spacing, spinning resulted in a diameter of 430.46 ± 118.19 nm, with a fibre homogeneity (σ) of 0.26. With increasing spacing, the fibre diameter decreases from 667 ± 83 nm at spacing 100 and 667 ± 83 nm for spacing 125, and the nanofiber is still considered homogeneous (σ<0.26).

Similar results were also observed in studies on PVP/CA electrospun fibres, where more uniform fibres with increased size were made with increased PVP content(Jauhari et al., 2019). The flying time and electric field strength greatly influence the electrospinning process and the resulting fibres. The distance tip between the tip and collector is essential in determining the flying time and electric field strength(Sorkhabi et al., 2022). As the distance between the tip and collector decreases, the jet has a shorter distance tip before reaching the collector plate. This increases the electric field strength, causing the jet to accelerate to the collector, resulting in less time for the solvent to evaporate. This results in a larger fibre diameter(Chinnappan, Krishnaswamy, Xu, & Hoque, 2022). The excess solvent can cause the fibres to coalesce when the distance is too low, forming inter- and intra-layer junctions and bonds.

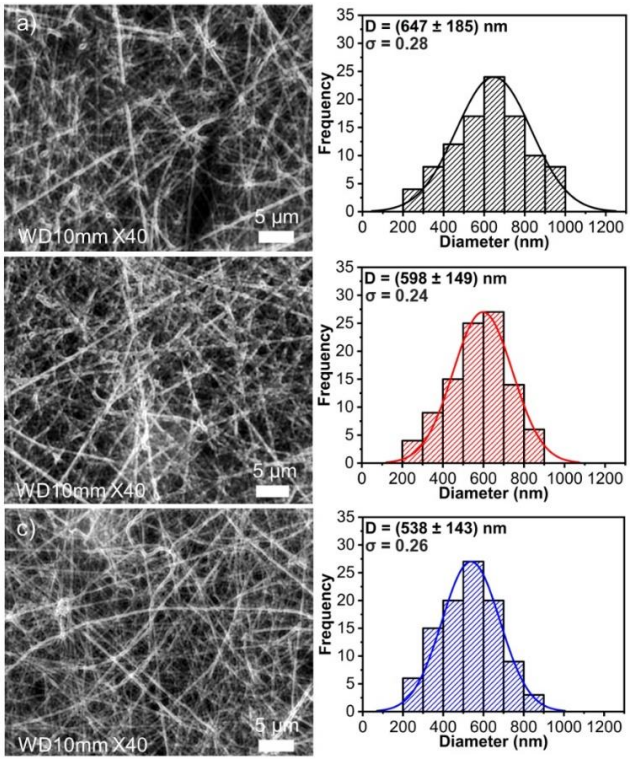

Figure 5. Morphology and Distribution of PVDF/PAN Composite Nanofiber of (a)PN3: 75 mm, (b)PN3: 100 mm dan (c)PN3: 125 mm as the Effect of distance of needle to collector Variables.

FTIR Analysis

The PVDF/PAN nanofiber composite produced five peak changes. The FTIR spectra between 550 and 3700 cm-1 are presented in Figure 6. The first in the range of 3700-3500 and 3000-2800 cm-1 represents the strong interaction of N-H stretching and C-H stretching(Emam, Elezaby, Swidan, Loutfy, & Hathout, 2023; Singh et al., 2020; Weret et al., 2020). A higher increase in PAN concentration led to sharper peaks, and the spectrum shifted to a higher wave number at 2245 cm-1, which was attributed to stretching in C≡N(Nadirah, Ong, Saheed, Yusof, & Shukur, 2020; C. Zhang et al., 2019). These peaks were typical characteristics derived from PAN spectra(Jauhari et al., 2021). Secondly, the absorption band located at 1404 cm-1 is related to C-F stretching vibrations, and the last peak is due to C-C bonding as well as weak peaks around 510 and 486 cm-1 attributed to CF_2 bending vibrations, which are derived from PVDF(Lim & Shin, 2020).

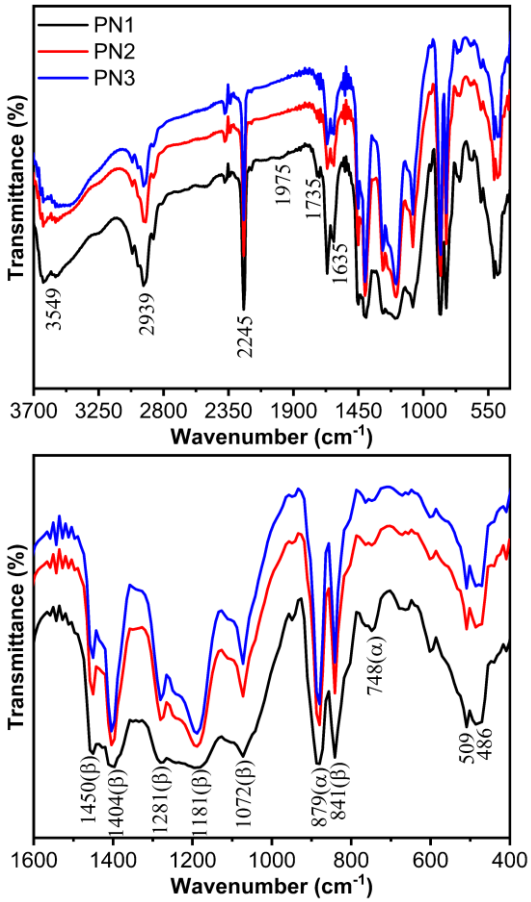

Figure 6. FTIR Analysis of nanofiber PN1, PN2, and PN3 loaded composite nanofiber.

Third, the peak around 1670 cm^{-1} is due to the oxidation of PAN in air, which results in the formation of a C=O double bond (Guo, Cheng, Huo, Ren, & Liu, 2020). The peaks around 1251 and 1360 cm^{-1} are derived from vibrations of aliphatic CH bonds of various modes in CH and CH_2(Weret et al., 2020), respectively. Fourth, the C=O band around 1735 cm^{-1} and the N=C-N amine group at 1635 cm^{-1} indicate the successful grafting of PAN in the PVDF matrix on the nanofiber surface(Kishore Chand et al., 2022). Finally, the influence of the PVDF phase is seen from the bands around 879, and 784cm-1 representing the α-phase(Gade et al., 2021;

Koç, Paralı, & Şan, 2020), and β-phase (~1450, 1404, 1181, 1072, 841 cm^{-1}))(Černohorský et al., 2021). The strong peak at 879 cm^{-1} was determined as the dominant α-phase, especially in PN2 and PN3 nanofibers. PAN concentration substantially affected the peaks for PVDF/PAN nanofibers, and the intensity decreased with increasing PAN content due to the chemical interaction of PVDF and PAN.

XRD Analysis

XRD was performed to confirm the crystal structure of the nanofiber. The PVDF/PAN nanofiber in the 2θ range of 5-60° is shown in Figure 7. The broad reflection in the 2θ range of 11.0°-37.0° is due to the amorphous nature of PVDF/PAN nanofiber. Nanofiber PN1 (15.22 Å) shows the weakest peaks where the background of PVDF (21.24° and 36.38°) and PAN (17.66 and 24.12°) are still detectable which represent characteristic reflections as characteristic reflections of (112), (220), (002) and (201) planes, respectively(Khalil, Aboamera, Nasser, Mahmoud, & Mohamed, 2019; Mousa, Fahmy, Abouzeid, Abdel-Jaber, & Ali, 2022; Singh et al., 2020; S. Zhang, Zhang, Zhang, & Ren, 2021). The XRD pattern of PN2 (16.66 Å) is characterized by peaks at 17.86° and 20.52° indicating characteristic reflections of the (200) and (011) planes, a reflection at 23.84° corresponding to the (220) plane and another reflection observed at 37.52° (132) (Bhute & Kondawar, 2019; Chen et al., 2022; Khalil et al., 2019; Ryšánek et al., 2019). A strong peak pattern of Nanofiber PN3 (26.66 Å) was found at 2θ due to reflections at 17.36° (102) and 23.98° (211), confirming the presence of PAN(Jauhari et al., 2021).

The crystallinity of the sample was calculated with Origin Pro 2023 software by comparing the crystalline area fraction to the whole spectra's area fraction (Almafie et al., 2022). PN1 showed a degree of crystallinity of 50.83%. The crystallinity of PN2 and PN3 was 43.23% and 40.94%, respectively; the crystallinity is likely due to the broken crystal lattice, giving a more amorphous structure. The electrospinning process transforms PVDF/PAN from a crystalline state to an amorphous state. Solutions undergo elongation, solvent evaporation, and liquid-to-solid transition simultaneously, preventing molecular reorientation between PVDF and PAN, resulting in lower-order molecules(Sriyanti et al., 2017). PVDF belongs to polycrystalline polymers with three distinct crystalline phases (α, β, and γ). The α-PVDF crystal phase is around 15.26°, 16.78°, and 18.16° derived from pure PVDF (Mahdavi Varposhti et al., 2020). The β crystalline phase is around 20.52°, and 23.32°, which may be due to the influence of the amorphous halo of PAN. In some reports, the electrospinning method can easily produce the β phase(Dang et al., 2020; He et al., 2021; Jin et al., 2020). However, our findings show a tendency of α phase dominance. This may be because a small amount of β phase coexists with α, or the interaction of PAN molecules prevents the formation of β phase. This finding corroborates our argument about the molecular interactions described in the FTIR analysis.

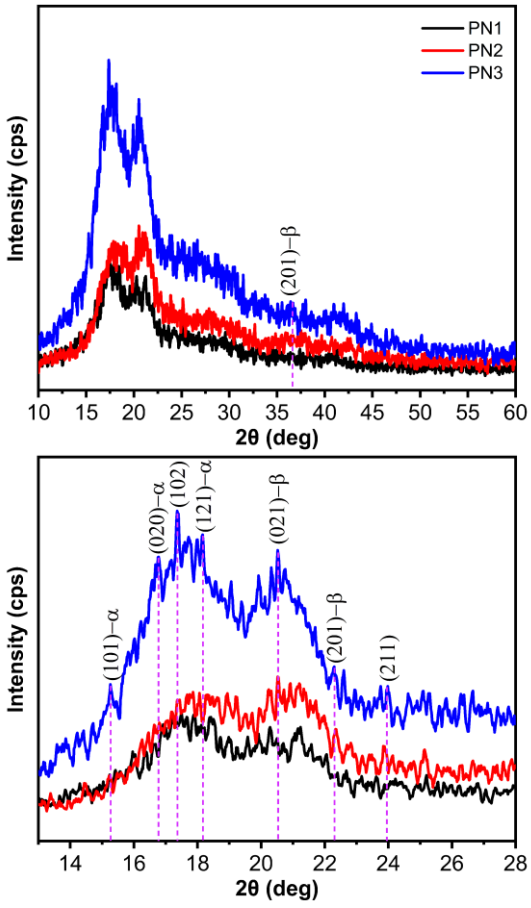

Figure 7. XRD Spectra of nanofiber PN1, PN2, and PN3 loaded composite nanofiber.

Conclusion

The nanofiber of PVDF/PAN were in the diameter range of 394-851 nm and 513-663 nm, respectively. The optimal state was at a solution of PN2: PAN 10% (w/w) and PVDF 6% (w/w), High Voltage 12 kV, Flow Rate PN3: 60 µl/min, and Needle to Collector Distance 75 mm. FTIR results showed substantial interaction where PAN was successfully grafted to the PVDF matrix characterized by peak changes and decreasing intensity. XRD results showed that the PVDF/PAN nanofiber was amorphized with less than 50.83% crystallinity.

Acknowledgments

This research was financially supported by Ministry of Education, Culture, Research, and Technology Republic of Indonesia under Fundamental Research – Regular contract, No.: 164/E5/PG.02.00/PL/2023, and Dev. contract No. 0144.07/UN9/SB3.LP2M.PT/2023.

Author Contributions

Ida Sriyanti: Conceptualization, Writing-Review & Editing, and Supervision, Project administration, Funding acquisition. Muhammad Rama Almafie: Writing-Original Draft, Formal analysis, Data Curation. Rahma Dani and Radiyati Umi Partan: Formal analysis, M Rudi Sanjaya and Jaidan Jauhari: Supervision of diameter with origin.

Conflicts of Interest

The authors declare that they have no known competing financial interests or personal relationships that could have appeared to influence the work reported in this paper.

References

Agarwal, S., Greiner, A., & Wendorff, J. H. (2013). Functional materials by electrospinning of polymers. *Progress in Polymer Science*, *38*, 963–991. https://doi.org/10.1016/j.progpolymsci.2013.02.001

Ahmadian, A., Shafiee, A., Aliahmad, N., & Agarwal, M. (2021). Overview of Nano-Fiber Mats Fabrication via Electrospinning and Morphology Analysis. *Textiles*, 1, 206–226. https://doi.org/10.3390/textiles1020010

Al-Abduljabbar, A., & Farooq, I. (2023). Electrospun Polymer Nanofibers: Processing, Properties, and Applications. *Polymers*, *15*(1). https://doi.org/10.3390/polym15010065

Al-Husaini, I. S., Lau, W. J., Yusoff, A. R. M., Al-Abri, M. Z., & Farsi, B. A. Al. (2021). Synthesis of functional hydrophilic polyethersulfone-based electrospun nanofibrous membranes for water treatment. *Journal of Environmental Chemical Engineering*, *9*(1), 104728. https://doi.org/10.1016/j.jece.2020.104728

Almafie, M. R., Marlina, L., Riyanto, R., Jauhari, J., Nawawi, Z., & Sriyanti, I. (2022). Dielectric Properties and Flexibility of Polyacrylonitrile/Graphene Oxide Composite Nanofibers. *ACS Omega*, *7*(37), 33087–33096. https://doi.org/10.1021/acsomega.2c03144

Baykara, T., & Taylan, G. (2021). Coaxial electrospinning of PVA/Nigella seed oil nanofibers: Processing and morphological characterization. *Materials Science and Engineering: B*, 265, 115012. https://doi.org/https://doi.org/10.1016/j.mseb.2020.115012

Bhute, M. V, & Kondawar, S. B. (2019). Electrospun poly(vinylidene fluoride)/cellulose acetate/AgTiO2 nanofibers polymer electrolyte membrane for lithium ion battery. *Solid State Ionics*, *333*, 38–44. https://doi.org/https://doi.org/10.1016/j.ssi.2019.01.019

Černohorský, P., Pisarenko, T., Papež, N., Sobola, D., Ţălu, Ş., Částková, K., … Sedlák, P. (2021). Structure Tuning and Electrical Properties of Mixed PVDF and Nylon Nanofibers. *Materials*, Vol. 14. https://doi.org/10.3390/ma14206096

Chen, P., Chai, M., Mai, Z., Liao, M., Xie, X., Lu, Z., … Zhou, W. (2022). Electrospinning polyacrylonitrile (PAN) based nanofiberous membranes synergic with plant antibacterial agent and silver nanoparticles (AgNPs) for potential wound dressing. *Materials Today Communications*, *31*, 103336. https://doi.org/https://doi.org/10.1016/j.mtcomm.2022.103336

Chinnappan, B. A., Krishnaswamy, M., Xu, H., & Hoque, M. E. (2022). Electrospinning of Biomedical Nanofibers/Nanomembranes: Effects of Process Parameters. *Polymers*, Vol. 14. https://doi.org/10.3390/polym14183719

Collins, G., Federici, J., Imura, Y., & Catalani, L. H. (2012). Charge generation, charge transport, and residual charge in the electrospinning of polymers: A review of issues and complications. *Journal of Applied Physics*, *111*(4). https://doi.org/10.1063/1.3682464

Dang, W., Liu, J., Wang, X., Yan, K., Zhang, A., Yang, J., … Liang, J. (2020). Structural transformation of polyacrylonitrile (PAN) fibers during rapid thermal pretreatment in nitrogen atmosphere. *Polymers*, *12*(1). https://doi.org/10.3390/polym12010063

Emam, M. H., Elezaby, R. S., Swidan, S. A., Loutfy, S. A., & Hathout, R. M. (2023). Cerium Oxide Nanoparticles/Polyacrylonitrile Nanofibers as Impervious Barrier against Viral Infections. *Pharmaceutics*, Vol. 15. https://doi.org/10.3390/pharmaceutics15051494

Eren Boncu, T., Ozdemir, N., & Uskudar Guclu, A. (2020). Electrospinning of linezolid loaded PLGA nanofibers: effect of solvents on its spinnability, drug delivery, mechanical properties, and antibacterial activities. *Drug Development and Industrial Pharmacy*, *46*(1), 109–121. https://doi.org/10.1080/03639045.2019.1706550

Gade, H., Nikam, S., Chase, G. G., & Reneker, D. H. (2021). Effect of electrospinning conditions on β-phase and surface charge potential of PVDF fibers. *Polymer*, *228*, 123902. https://doi.org/https://doi.org/10.1016/j.polymer.2021.123902

Gelb, M. B., Punia, A., Sellers, S., Kadakia, P., Ormes, J. D., Khawaja, N. N., … Lamm, M. S. (2022). Effect of drug incorporation and polymer properties on the characteristics of electrospun nanofibers for drug delivery. *Journal of Drug Delivery Science and Technology*, *68*, 103112. https://doi.org/https://doi.org/10.1016/j.jddst.2022.103112

Ghafouri, S. E., Mousavi, S. R., Khakestani, M., Mozaffari, S., Ajami, N., & Khonakdar, H. A. (2022). Electrospun nanofibers of poly (lactic acid)/poly (ε-caprolactone) blend for the controlled release of levetiracetam. *Polymer Engineering & Science*, *62*(12), 4070–4081. https://doi.org/https://doi.org/10.1002/pen.26167

Guo, Y., Cheng, C., Huo, T., Ren, Y., & Liu, X. (2020). Highly effective flame retardant lignin/polyacrylonitrile composite prepared via solution blending and phosphorylation. *Polymer Degradation and Stability*, *181*, 109362. https://doi.org/https://doi.org/10.1016/j.polymdegradstab.2020.109362

He, Z., Rault, F., Lewandowski, M., Mohsenzadeh, E., & Salaün, F. (2021). Electrospun PVDF Nanofibers for Piezoelectric Applications: A Review of the Influence of Electrospinning Parameters on the β Phase and Crystallinity Enhancement. *Polymers*, Vol. 13. https://doi.org/10.3390/polym13020174

Ince Yardimci, A., Durmus, A., Kayhan, M., & Tarhan, O. (2022). Antibacterial Activity of AgNO3 Incorporated Polyacrylonitrile/Polyvinylidene Fluoride (PAN/PVDF) Electrospun Nanofibrous Membranes and Their Air Permeability Properties. *Journal of Macromolecular Science, Part B*, *61*(6), 749–762. https://doi.org/10.1080/00222348.2022.2101970

Islam, M. S., Ang, B. C., Andriyana, A., & Afifi, A. M. (2019). A review on fabrication of nanofibers via electrospinning and their applications. *SN Applied Sciences*, *1*(10), 1–16. https://doi.org/10.1007/s42452-019-1288-4

Jadbabaei, S., Kolahdoozan, M., Naeimi, F., & Ebadi-Dehaghani, H. (2021). Preparation and characterization of sodium alginate–PVA polymeric scaffolds by electrospinning method for skin tissue engineering applications. *RSC Advances*, *11*(49), 30674–30688. https://doi.org/10.1039/D1RA04176B

Jauhari, J., Suharli, A. J., Nawawi, Z., & Sriyanti, I. (2021). Synthesis and Characteristics of Polyacrylonitrile (Pan) Nanofiber Membrane Using Electrospinning Method. *Journal of Chemical Technology and Metallurgy*, *56*(4), 698–703.

Jauhari, J., Wiranata, S., Rahma, A., Nawawi, Z., & Sriyanti, I. (2019). Polyvinylpyrrolidone/cellulose acetate nanofibers synthesized using electrospinning method and their characteristics. *Materials Research Express*, *6*(6), 64002. https://doi.org/10.1088/2053-1591/ab0b11

Jiang, J., Zheng, G., Wang, X., Li, W., Kang, G., Chen, H., … Liu, J. (2020). Arced Multi-Nozzle Electrospinning Spinneret for High-Throughput Production of Nanofibers. *Micromachines*, Vol. 11. https://doi.org/10.3390/mi11010027

Jin, L., Zheng, Y., Liu, Z.-K., Li, J.-S., Yi, Y.-P.-Q., Fan, Y.-Y., … Li, Y. (2020). Enhancement of β-Phase Crystal Content of Poly(vinylidene fluoride) Nanofiber Web by Graphene and Electrospinning Parameters. *Chinese Journal of Polymer Science*, *38*(11), 1239–1247. https://doi.org/10.1007/s10118-020-2428-4

Julius, H. F. S. S. D. R. ,. (2012). APPLICATION OF PIEZOELECTRIC MATERIAL FILM PVDF (Polyvinylidene Flouride) AS LIQUID VISCOSITY SENSOR. *Jurnal Neutrino*, *3*(2), 129–142. https://doi.org/10.18860/neu.v0i0.1648

Kenry, & Lim, C. T. (2017). Nanofiber technology: current status and emerging developments. *Progress in Polymer Science*, *70*, 1–17. https://doi.org/10.1016/j.progpolymsci.2017.03.002

Khalil, A., Aboamera, N. M., Nasser, W. S., Mahmoud, W. H., & Mohamed, G. G. (2019). Photodegradation of organic dyes by PAN/SiO2-TiO2-NH2 nanofiber membrane under visible light. *Separation and Purification Technology*, *224*, 509–514. https://doi.org/https://doi.org/10.1016/j.seppur.2019.05.056

Khan, I., Saeed, K., & Khan, I. (2019). Nanoparticles: Properties, applications and toxicities. *Arabian Journal of Chemistry*, *12*(7), 908–931. https://doi.org/10.1016/j.arabjc.2017.05.011

Kishore Chand, A. A., Bajer, B., Schneider, E. S., Mantel, T., Ernst, M., Filiz, V., & Glass, S. (2022). Modification of Polyacrylonitrile Ultrafiltration Membranes to Enhance the Adsorption of Cations and Anions. *Membranes*, Vol. 12. https://doi.org/10.3390/membranes12060580

Koç, M., Paralı, L., & Şan, O. (2020). Fabrication and vibrational energy harvesting characterization of flexible piezoelectric nanogenerator (PEN) based on PVDF/PZT. *Polymer Testing*, *90*, 106695. https://doi.org/https://doi.org/10.1016/j.polymertesting.2020.106695

Kusumawati, D. H., Istiqomah, K. V. N., Husnia, I., & Fathurin, N. (2021). Synthesis of nanofiber polyvinyl alcohol (PVA) with electrospinning method. *Journal of Physics: Conference Series*, *2110*(1). https://doi.org/10.1088/1742-6596/2110/1/012010

Latiffah, E., Agung, B. H., Hapidin, D. A., & Khairurrijal, K. (2022). Fabrication of Polyvinylpyrrolidone (PVP) Nanofibrous Membranes using Mushroom-Spinneret Needleless Electrospinning. *Journal of Physics: Conference Series*, *2243*(1). https://doi.org/10.1088/1742-6596/2243/1/012101

Lee, S., Bui-Vinh, D., Baek, M., Kwak, D. Bin, & Lee, H. (2023). Modeling pressure drop values across ultra-thin nanofiber filters with various ranges of filtration parameters under an aerodynamic slip effect. *Scientific Reports*, *13*(1), 1–14. https://doi.org/10.1038/s41598-023-32765-4

Li, Y., Liao, C., & Tjong, S. C. (2019). Electrospun polyvinylidene fluoride-based fibrous scaffolds with piezoelectric characteristics for bone and neural tissue engineering. *Nanomaterials*, *9*(7). https://doi.org/10.3390/nano9070952

Liang, Q., Pan, W., & Gao, Q. (2021). Preparation of carboxymethyl starch/polyvinyl-alcohol electrospun composite nanofibers from a green approach. *International Journal of Biological Macromolecules*, *190*, 601–606. https://doi.org/https://doi.org/10.1016/j.ijbiomac.2021.09.015

Lim, S. J., & Shin, I. H. (2020). Graft copolymerization of GMA and EDMA on PVDF to hydrophilic surface modification by electron beam irradiation. *Nuclear Engineering and Technology*, *52*(2), 373–380. https://doi.org/https://doi.org/10.1016/j.net.2019.07.018

Liyanage, A. A. H., Biswas, P. K., Dalir, H., & Agarwal, M. (2023). Engineering uniformity in mass production of MWCNTs/epoxy nanofibers using a lateral belt-driven multi-nozzle electrospinning technique to enhance the mechanical properties of CFRPs. *Polymer Testing*, *118*, 107883. https://doi.org/https://doi.org/10.1016/j.polymertesting.2022.107883

Machín, A., Fontánez, K., Arango, J. C., Ortiz, D., De León, J., Pinilla, S., … Márquez, F. (2021). One-dimensional (1d) nanostructured materials for energy applications. *Materials*, *14*(10). https://doi.org/10.3390/ma14102609

Mahdavi Varposhti, A., Yousefzadeh, M., Kowsari, E., & Latifi, M. (2020). Enhancement of β-Phase Crystalline Structure and Piezoelectric Properties of Flexible PVDF/Ionic Liquid Surfactant Composite Nanofibers for Potential Application in Sensing and Self-Powering. *Macromolecular Materials and Engineering*, *305*(3), 1900796. https://doi.org/https://doi.org/10.1002/mame.201900796

Mohseni, M., Delavar, F., & Rezaei, H. (2021). The piezoelectric gel-fiber-particle substrate containing short PVDF-chitosan-gelatin nanofibers and mesoporous silica nanoparticles with enhanced antibacterial activity as a potential of wound dressing applications. *Journal of Macromolecular Science, Part A: Pure and Applied Chemistry*, *58*(10), 694–708. https://doi.org/10.1080/10601325.2021.1927754

Mousa, H. M., Fahmy, H. S., Abouzeid, R., Abdel-Jaber, G. T., & Ali, W. Y. (2022). Polyvinylidene fluoride-cellulose nanocrystals hybrid nanofiber membrane for energy harvesting and oil-water separation applications. *Materials Letters*, *306*, 130965. https://doi.org/https://doi.org/10.1016/j.matlet.2021.130965

Nadirah, B. N., Ong, C. C., Saheed, M. S. M., Yusof, Y. M., & Shukur, M. F. (2020). Structural and conductivity studies of polyacrylonitrile/methylcellulose blend based electrolytes embedded with lithium iodide. *International Journal of Hydrogen Energy*, *45*(38), 19590–19600. https://doi.org/https://doi.org/10.1016/j.ijhydene.2020.05.016

Prabu, G. T. V, & Dhurai, B. (2020). A Novel Profiled Multi-Pin Electrospinning System for Nanofiber Production and Encapsulation of Nanoparticles into Nanofibers. *Scientific Reports*, *10*(1), 4302. https://doi.org/10.1038/s41598-020-60752-6

Rathore, P., & Schiffman, J. D. (2021). Beyond the Single-Nozzle: Coaxial Electrospinning Enables Innovative Nanofiber Chemistries, Geometries, and Applications. *ACS Applied Materials & Interfaces*, *13*(1), 48–66. https://doi.org/10.1021/acsami.0c17706

Reneker, D. H., Yarin, A. L., Fong, H., & Koombhongse, S. (2000). Bending instability of electrically charged liquid jets of polymer solutions in electrospinning. *Journal of Applied Physics*, *87*(9 I), 4531–4547. https://doi.org/10.1063/1.373532

Russo, F., Ursino, C., Avruscio, E., Desiderio, G., Perrone, A., Santoro, S., … Figoli, A. (2020). Innovative poly (Vinylidene fluoride) (PVDF) electrospun nanofiber membrane preparation using DMSO as a low toxicity solvent. *Membranes*, *10*(3), 1–17. https://doi.org/10.3390/membranes10030036

Ryšánek, P., Benada, O., Tokarský, J., Syrový, M., Čapková, P., & Pavlík, J. (2019). Specific structure, morphology, and properties of polyacrylonitrile (PAN) membranes prepared by needleless electrospinning; Forming hollow fibers. *Materials Science and Engineering: C*, *105*, 110151. https://doi.org/https://doi.org/10.1016/j.msec.2019.110151

Saha, S., Yauvana, V., Chakraborty, S., & Sanyal, D. (2019). Synthesis and characterization of polyvinylidene-fluoride (PVDF) nanofiber for application as piezoelectric force sensor. *Materials Today: Proceedings*, *18*, 1450–1458. https://doi.org/10.1016/j.matpr.2019.06.613

Sanchaniya, J. V., & Kanukuntla, S. (2023). Morphology and mechanical properties of PAN nanofiber mat.

Journal of Physics: Conference Series, *2423*(1). https://doi.org/10.1088/1742-6596/2423/1/012018

Sengor, M., Ozgun, A., Gunduz, O., & Altintas, S. (2020). Aqueous electrospun core/shell nanofibers of PVA/microbial transglutaminase cross-linked gelatin composite scaffolds. *Materials Letters*, *263*, 127233. https://doi.org/https://doi.org/10.1016/j.matlet.2019.127233

Singh, R., Janakiraman, S., Khalifa, M., Anandhan, S., Ghosh, S., Venimadhav, A., & Biswas, K. (2020). A high thermally stable polyacrylonitrile (PAN)-based gel polymer electrolyte for rechargeable Mg-ion battery. *Journal of Materials Science: Materials in Electronics*, *31*(24), 22912–22925. https://doi.org/10.1007/s10854-020-04818-1

Sorkhabi, T. S., Samberan, M. F., Ostrowski, K. A., Zajdel, P., Stempkowska, A., & Gawenda, T. (2022). Electrospinning of Poly (Acrylamide), Poly (Acrylic Acid) and Poly (Vinyl Alcohol) Nanofibers: Characterization and Optimization Study on the Effect of Different Parameters on Mean Diameter Using Taguchi Design of Experiment Method. *Materials*, Vol. 15. https://doi.org/10.3390/ma15175876

Sriyanti, I., Edikresnha, D., Rahma, A., Munir, M. M., Rachmawati, H., & Khairurrijal, K. (2017). Correlation between Structures and Antioxidant Activities of Polyvinylpyrrolidone/*Garcinia mangostana* L. Extract Composite Nanofiber Mats Prepared Using Electrospinning. *Journal of Nanomaterials*, *2017*, 9687896. https://doi.org/10.1155/2017/9687896

Sriyanti, I., Marlina, L., Fudholi, A., Marsela, S., & Jauhari, J. (2021). Physicochemical properties and In vitro evaluation studies of polyvinylpyrrolidone/cellulose acetate composite nanofibres loaded with Chromolaena odorata (L) King extract. *Journal of Materials Research and Technology*, *12*, 333–342. https://doi.org/https://doi.org/10.1016/j.jmrt.2021.02.083

Tan, S. H., Inai, R., Kotaki, M., & Ramakrishna, S. (2005). Systematic parameter study for ultra-fine fiber fabrication via electrospinning process. *Polymer*, *46*(16), 6128–6134. https://doi.org/10.1016/j.polymer.2005.05.068

Thorat, Y. V, Chavan, S. S., & Mohite, D. D. (2022). Electro spun PAN Nanofiber with Optimized Diameter. *Journal of Algebraic Statistics*, *13*(2), 1447–1454.

Wang, X., & Nakane, K. (2020). Preparation of polymeric nanofibers via immersion electrospinning. *European Polymer Journal*, *134*, 109837. https://doi.org/https://doi.org/10.1016/j.eurpolymj.2020.109837

Weret, M. A., Jeffrey Kuo, C.-F., Zeleke, T. S., Beyene, T. T., Tsai, M.-C., Huang, C.-J., … Hwang, B.-J. (2020). Mechanistic understanding of the Sulfurized-Poly(acrylonitrile) cathode for lithium-sulfur batteries. *Energy Storage Materials*, *26*, 483–493. https://doi.org/https://doi.org/10.1016/j.ensm.2019.11.022

Xu, L. (徐磊), Lv, J. (吕娇), Wang, X. (王翔), & Qu, W. (屈文涛). (2023). Wave propagation of bending jet in electrospinning process. *AIP Advances*, *13*(4), 45218. https://doi.org/10.1063/5.0126064

Xue, J., Wu, T., Dai, Y., & Xia, Y. (2019). Electrospinning and electrospun nanofibers: Methods, materials, and applications [Review-article]. *Chemical Reviews*, *119*(8), 5298–5415. https://doi.org/10.1021/acs.chemrev.8b00593

Zhang, C., Li, R., Liu, J., Guo, S., Xu, L., Xiao, S., & Shen, Z. (2019). Hydrogen peroxide modified polyacrylonitrile-based fibers and oxidative stabilization under microwave and conventional heating – The 1st comparative study. *Ceramics International*, *45*(10), 13385–13392. https://doi.org/https://doi.org/10.1016/j.ceramint.2019.04.035

Zhang, S., Zhang, B., Zhang, J., & Ren, K. (2021). Enhanced Piezoelectric Performance of Various Electrospun PVDF Nanofibers and Related Self-Powered Device Applications. *ACS Applied Materials & Interfaces*, *13*(27), 32242–32250. https://doi.org/10.1021/acsami.1c07995